Journal of Advanced Mechanical Design, Systems, and Manufacturing

Vol.2, No.2, 2008

Development of SCARA-Type Haptic Device for Electrostatic Non-Contact Handling System*

Ewoud van WEST**, Akio YAMAMOTO**, Benjamin BURNS***
and Toshiro HIGUCHI**

** Advanced Mechatronics Laboratory, Department of Precision Engineering,
School of Engineering, the University of Tokyo
7–3–1 Hongo, Bunkyo-ku, Tokyo 113-8656, Japan
E-mail: [ewoud, akio, higuchi]@aml.t.u-tokyo.ac.jp

*** Laboratoire de Systèmes Robotiques, Ecole Polytechnique Fédérale de Lausanne
Station 9, CH-1015 Lausanne, Switzerland
E-mail: benjamin.burns@epfl.ch

Abstract

This paper describes the development of a SCARA-type haptic device, which will be used to assist a human operator in non-contact object handling of silicon wafers using electrostatic levitation. The device has three degrees of freedom, of which only one (vertical) is actively controlled. By utilizing the admittance control paradigm, a high vertical stiffness and a high output force can be achieved. These properties are necessary for the intended application of non-contact object handling to prevent instabilities (induced by the human motion) of the electrostatic levitation system. As the nominal air gap between object and electrostatic levitator is in the order of 350 micrometer, with an allowable position error of about 150 micrometer, instability can easily occur if there is no haptic assistance, especially in the picking up or placing process. The developed SCARA-type haptic device has a mechanical stiffness of 51 N/mm for the vertical direction when it is in the weakest posture, which is sufficient for the non-contact handling task. The design and performance of the haptic device for the active vertical degree of freedom are described in this paper.

Key words : SCARA, Haptic, Haptic Tweezer, Pick and Place, Man Machine Interface

1. Introduction

Haptic devices are mostly used for tele-operation tasks[1] and virtual reality applications[2] as they can restore, create, or enhance the sensation of touch, which was lost or diminished in these applications. However, the force or displacement capabilities of haptic devices can also be used in a more active way by assisting in a practical task, e.g. human power amplification.[3] Furthermore, tactile sensation is very intuitive and it does not require any interpretation, so that haptic assistance while performing a difficult task, can augment the human performance.[4] A nice example of such human machine collaborative haptics can be found in assisted surgery with the steady-hand.[5] Here, the haptic device actively reduces tremors coming from the surgeon's hand and performance during surgery can be improved.

Human machine collaborative haptics has also been applied to a non-contact handling system for contact sensitive objects[6] in a concept called: "Haptic Tweezer". In this concept, which is also illustrated in Fig. 1, a human operator performs a pick and place task of a delicate object, e.g. silicon wafer, without making any contact between tool and object. By using levitation techniques, such as magnetic and electrostatic levitation, the object is suspended by an attractive force from a levitator that balances the gravitational force at a certain air gap between levitator and object. Because there is no mechanical contact between levitator and object, problems such as contamination and damage, which can be present in conventional

*Received 1 Oct., 2007 (No. 07-0605)
[DOI: 10.1299/jamdsm.2.180]

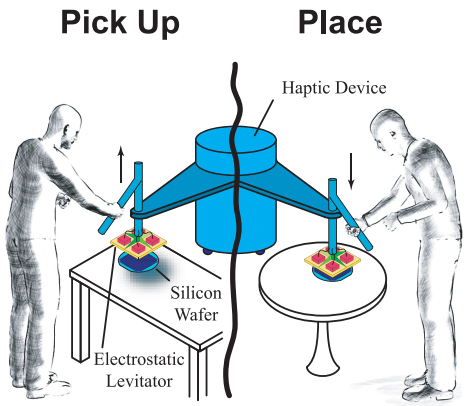
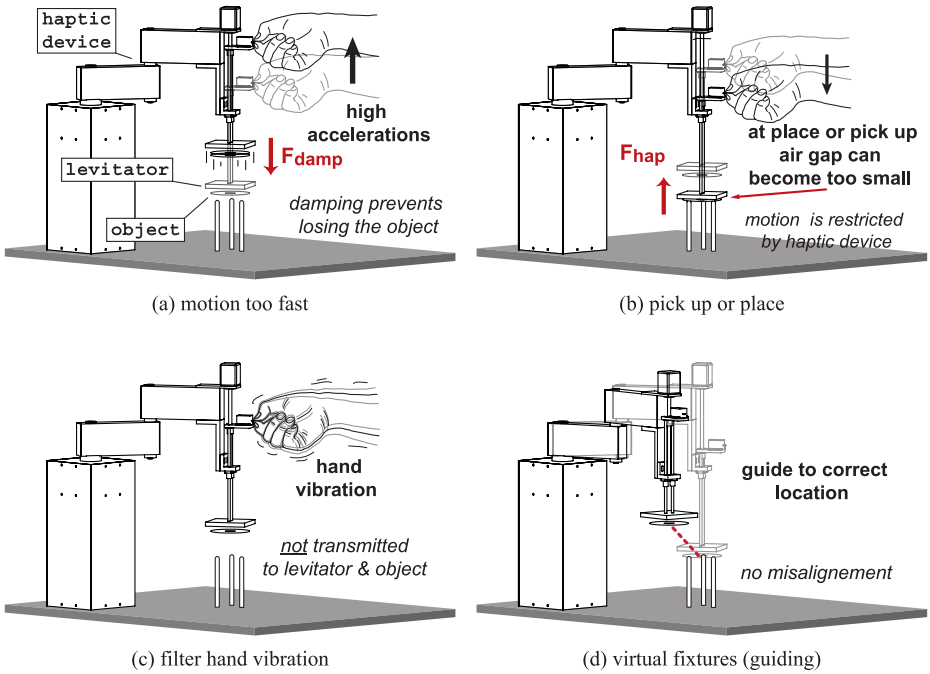


Fig. 1 Concept of Haptic Tweezer



(a) motion too fast

(b) pick up or place

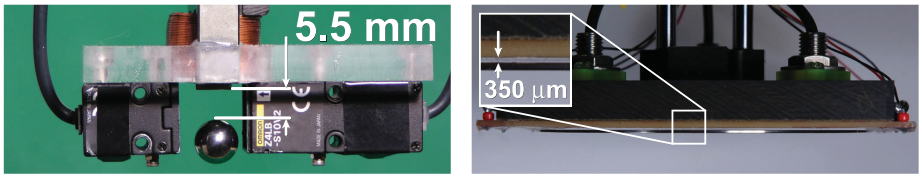
(c) filter hand vibration

(d) virtual fixtures (guiding)

Fig. 2 Examples of Haptic Tweezer

handling systems (e.g. carrier spatula), are prevented.

However, non-contact handling is much more sensitive to disturbances, especially when they are induced by the operator. The haptic device can in real time compensate or regulate these disturbances by giving active feedback to the operator. Some examples of what the haptic device can do in this "Haptic Tweezer" concept, are illustrated in Fig. 2, where the operator is holding the haptic device with the levitator as end-effector. In Fig. 2(a), a high acceleration from the operator's hand is damped to prevent that the object can not follow the high acceleration and drop. The same holds for the reverse case of high deceleration. Fig. 2(b) shows how for the actual picking up and placing of the object, the human motion can easily force the object to touch the levitator as the air gap between object and levitator is small. The haptic device can restrict such motion by for example exerting a force to counteract the operator's motion and maintain the air gap between object and levitator. Other means to improve non-contact handling performance, which are not unique to the Haptic Tweezer concept, can include hand vibration isolation as shown in Fig. 2(c) and the use of virtual fixtures as shown in Fig. 2(d), which can guide to operator to follow a preferred path.



(a) Magnetic levitation of iron ball (b) Electrostatic levitation of aluminum disk

Fig. 3 Typical air gap for different levitation systems

The beneficial aspects of this concept were demonstrated using a prototype based on the haptic device PHANToM Omni (Sensable Technologies) and a magnetic levitation system[6] and it showed the beneficial aspects of the collaborative system especially during picking up and placing. However, for a more useful non-contact handling tool, the use of electrostatic levitation is better as it can levitate not only conducting materials,[7] but also semiconductors,[8] and dielectrics.[9] However, a drawback of electrostatic levitation is the weak levitation force and a small air gap. This difference in air gap between a typical magnetic levitation and a typical electrostatic levitation system is shown in Fig. 3. As a consequence of this smaller air gap in electrostatic levitation, the requirements on especially stiffness of the haptic device are much higher (considering the situation in Fig. 2(b)). Therefore, a suitable haptic device, which can be combined in a non-contact collaborative handling tool that uses electrostatic levitation, has to be found or developed. This paper reports the development of a new haptic device, which has the general structure of a SCARA-type robot[10] and that is specifically designed to be used in an electrostatic non-contact handling tool. The haptic device has three degrees of freedom (DOF) of which one is actively controlled (the vertical up and down motion), while the other two rotational DOF provide the necessary workspace passively.

The order of this manuscript is as follows. Section 2 describes different types of haptic devices and why the reported haptic device is based on a SCARA-type robot and uses the admittance control strategy. Next, Section 3 gives an overview of the design and realization of the SCARA-type haptic device, which includes hardware, control, and software. The performance of the haptic device is given in Section 4. Finally, in Section 5 final conclusions are given regarding the developed prototype.

2. Haptic Devices

This section will describe briefly the two distinct classes of haptic devices, namely impedance controlled devices and admittance controlled devices. It also explains why a SCARA-type haptic device based on the admittance control strategy is suitable for the electrostatic non-contact handling tool.

2.1. Impedance and admittance controlled devices

Haptic devices can be categorized in two distinct classes: impedance controlled devices and admittance controlled devices. As the naming implies, they are the inverse of each other. The inverse characteristics are not only visible from a control point of view, they are also reflected in the mechanical design and hence the performance.

The impedance controlled haptic devices have the following strategy: the haptic devices measures the position from the operator and feeds back a proper force to the operator based on a virtual model (position in, force out). The virtual model basically represents a force equation that relates the input (in this case position) to the output of the device (force) and some basic elements that can be included are inertia, spring behavior, damping, friction, etc. The operator experiences these elements in the interaction with the haptic device. For example, the virtual touching of a soft object can be created by making a damped one-directional spring around a certain position (where the soft object is touched). So, by selecting different elements in this virtual model, a great variety of virtual experiences can be made.

In the case of impedance controlled haptic devices however, the real inertia and friction of the haptic device itself can always be felt by the operator, which influences the haptic experience. Therefore in the design of impedance controlled haptic devices, the design has typically lightweight and highly back-drivable properties. A drawback of this strategy is that it limits the performance of the device in terms of realizable stiffness, and also the force output is typically not very high. However, for rendering low mass and stiffness, the admittance controlled device is very suitable. Perhaps the most famous examples of impedance controlled haptic devices are the commercial available PHANToM series from Sensable Technologies.[2]

Admittance controlled haptic devices have the inverse control strategy of impedance controlled devices: the haptic device measures a force from the operator and outputs a proper position based on a virtual model (force in, position out). The virtual model works the same way as described for admittance controlled haptic devices, where the only difference is that now input and output are inverted. As in this strategy, the friction of the haptic device itself is reduced by the control strategy, the devices are typically more robust and can output higher forces compared to impedance controlled devices. Even industrial robots fitted with a force sensor, can be used as haptic devices.[11] However, the performance in rendering low mass is typically not good as it requires high accelerations and speed from the device which can not always be realized. A nice example of an admittance controlled commercially available haptic device is the HapticMaster.[12]

2.2. Haptic device and non-contact handling tool

One of the most important criteria for selecting the right haptic device when combining it with a levitation system as like the "Haptic Tweezer" concept, is the stiffness it can realize. This can be best understood by considering the situation as shown in Fig. 2(b). Here, the operator wants to place a disk (representing a silicon wafer) on a certain position. Initially, there is an air gap between disk and levitator, which is realized by stable levitation. The operator moves both the levitator and the disk down and the air gap does not change. However, when the disk touches the desired location, the downwards motion from the operator will force the air gap between levitator and disk to become smaller. As the air gap should not become too small, a force from the haptic device (F_{hap}) is generated to stop the downward motion. The placing force (1 N order) and maximum allowable position error on the levitation system (150 μm order) will give a minimum stiffness that is required from the haptic device.

In the first prototype of the "Haptic Tweezer" concept, a magnetic levitation system as shown in Fig. 3(a) was combined with the admittance controlled haptic device PHANToM Omni for demonstrating the "Haptic Tweezer" concept in a pick and place task. Even though the force and stiffness of the PHANToM Omni is low (operating settings: F_{max} = 1.5 N, k = 360 N/m), it was sufficient to make a successful working prototype.

In case of electrostatic levitation, the allowable levitation position error is much smaller compared to the case of magnetic levitation (e.g. ±150 μm electrostatic, ±3 mm magnetic). This requires a much higher stiffness from the haptic device and therefore admittance controlled haptic devices will be more suitable. A structure that is frequently used in conventional pick and place application and which has a high mechanical stiffness in the vertical up and down direction is the SCARA robot. Therefore, this structure is used as a base point in the development of a new type haptic device that can be combined easily with electrostatic levitation for a collaborative non-contact handling tool.

3. Design and realization of SCARA-Type Haptic Device

This section will describe not only the design of the haptic device, but also the details of the realized prototype on control, hardware, and software are presented.

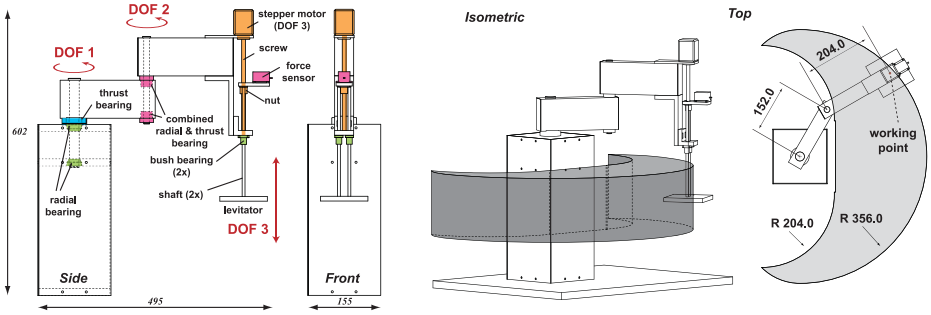


Fig. 4 Design and workspace of SCARA-type haptic device

3.1. Design

As the haptic device will be used for the specific task of non-contact object handling, it is necessary to know the requirements that are needed for this task. The following requirements were used as a guideline for the first prototype:

- High mechanical stiffness in vertical direction (order 10^4 N/m)
- Position resolution of at least 10 μm
- Vertical actuation force at least 10 N
- Workspace in the order of $300 \times 200 \times 150$ mm^3 (width $\times$ depth $\times$ height)

The first requirement of mechanical stiffness is based on the minimum stiffness that is needed to counteract a placing force of 1 N while not exceeding the allowable position error of the levitation system of 150 μm. With some safety margin, the desired mechanical stiffness is set to $1/(150 \cdot 10^{-6}) = 6.7 \cdot 10^3 \approx 10^4$ N/m order. For the second requirement of position resolution, it is desired that the step resolution is smaller than the levitation error of electrostatic levitation at steady state. This error (including noise signal), which can be observed during stable levitation does not exceed a 10 μm band around the setpoint. An actuation force of at least 10 N is required to counteract the human force exerted on the device. Even though this force is around 1 N in a precision handling task, it can exceed higher values (for example rough handling), so with safety margins the minimum requirement has been set to 10 N. Regarding the workspace, the prototype haptic device should allow the operator to pick up an object, move it away, and place it on another location. The selected values are a rough estimation of what motion ranges is needed to show a working prototype. Difference in the values for width and depth come from the natural difference of human motion for lateral and distal motions, while the height was selected as a value that gives enough initial clearance between object and device in the non-contact handling application.

The design that shows the general configuration of the SCARA-type haptic device is shown in Fig. 4 on the left side. The two rotational DOF are realized by a combination of thrust and radial bearings, which are highlighted in the figure. The vertical translation DOF is actively controlled by using a direct ball screw stepper motor combination, which means that the stepper motor is directly attached to the rotating screw. Advantages of this combination of ball screw and stepper motor is that it has no coupling and it is backlash free. The rotation of the stepper motor is therefore efficiently transformed in a translational motion at the nut. The translational motion is transferred to the levitator by two shafts, which are guided by two bush bearings. The center of the levitator is used as the central working point that can move around a workspace that is indicated in Fig. 4 on the right side. The angles are limited to 270° for the first DOF and 180° for the second DOF as in reality wires and cables from the stepper motor and levitator will prevent a full 360° rotation of both joints. The input force of the operator is measured by a force sensor that is attached to the moving part (at the nut).

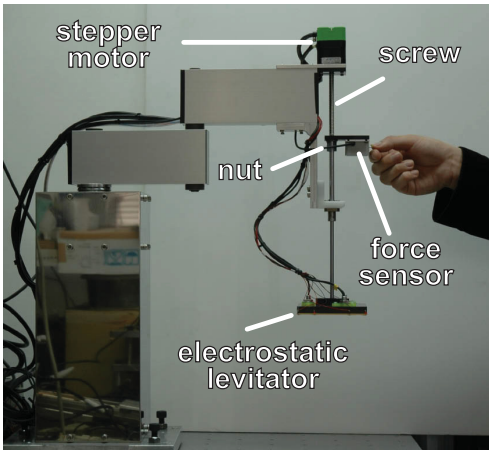


Fig. 5 Realized SCARA-type haptic device

Table 1 Specifications of position actuator

Stepper motor SiMB0802 specifications		
Stroke	160	mm
Lead	2	mm
Resolution	$7.8 \cdot 10^{-8}$	m
Thrust force	150	N
Specifications in controlled state (servo)		
Step resolution	8	μm
Maximum speed	80	mm/s
Delay time	3	ms

3.2. Realized device

The mechanical structure of the realized prototype is shown in Fig. 5. The base is a box-shaped structure constructed out of steel, while both the first and second link are constructed out of rectangular aluminum tubes. The links are connected to the base and each other by steel pins. At the end of the second link, the combination of stepper motor and ball screw is connected through an aluminum plate (top), an aluminum angle (bottom), and a Polyethylene (POM) angle (connected to the aluminum angle). This POM angle holds the rotational bearing for the ball screw, and the two bush bearings that guide the moving shafts.

The characteristics of the stepper motor ball screw combination (kSS SiMB0802) are described in Table 1. The manufacturer guarantees no step out of the motor and this is used in the position servo control of the motor as will be described in the next section. The motor will be driven through pulse command.

The force sensor is a strain-gage load cell (Kyowa LVS-1KA), which has a rated capacity of 10 N and it is mounted at a bakelite support plate that is attached to the nut.

3.3. Control & Software

The admittance control strategy of haptic device is given in Fig. 6 on the left side of the figure. The human operator exerts a force to the haptic device (measured by the force sensor) and this force is input to the virtual model. This virtual model defines the experience of the operator by relating the input force to an output position based on a force equation in which the desired virtual elements are present. The output position of the virtual model serves as a reference position Z_{ref} that should be followed by a servo controlled position actuator. The figure shows an example of a basic virtual model where there is only a virtual mass m_v for which motion is virtually damped by d_v. This virtual model allows to test in a easy way if the haptic device functions properly. Also, the model which will be used when the haptic device

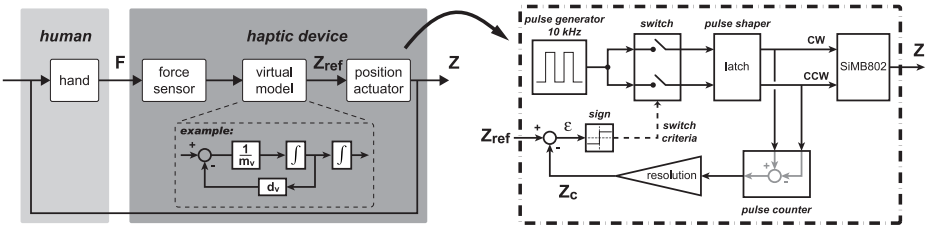


Fig. 6 Control strategy

is applied for contactless electrostatic transporting, has this simple model as a basis. Some of the parameters in the virtual model can be changed in real-time using ControlDesk (dSPACE). The final output of the the haptic device comes from the position actuator, which generates the real position Z that is ideally the same as Z_{ref}. This is also the motion which is felt by the human operator.

As the ball screw stepper motor that is used for the position actuator is driven by pulse command, a controller is implemented on a digital signal processing (DSP) system that is additional to the controller unit provided by the manufacturer of the stepper motor. Details of this additional controller are provided on the right side of Fig. 6. It has the general structure of feedback control. The reference position Z_{ref} has a negative feedback of the counted position Z_c which leads to a position error ε. Depending on the sign of this error, either positive or negative pulses will be generated to the stepper motor through a switch and a pulse generator. A pulse shaper is made to ensure that each pulse that is sent to the motor has the same time duration, as a switching command in the middle of a pulse can reduce the time duration. The pulses are counted and multiplied by the resolution to give the counted position. So, even though the real position is not measured, with the guarantee that no step out of the stepper motor occurs, reliable position control is realized, although it includes a positioning delay that exists in the SiMB controller. As the maximum pulse frequency that can be realized on the DSP is limited, a tradeoff between speed and accuracy has to be made in the selection of the step resolution. The DSP (dSPACE DS1104) is running at 20 kHz, so the maximum frequency of the pulse generator is fixed at 10 kHz (half). The maximum speed that can now be realized will depend on which resolution is set for the position actuator (maximum speed = pulse frequency × resolution). A step resolution has been selected of 8 μm, which gives a maximum speed of 80 mm/s that is sufficient for the intended haptic application while it is still below the desired requirement of 10 μm stated in Section 3.

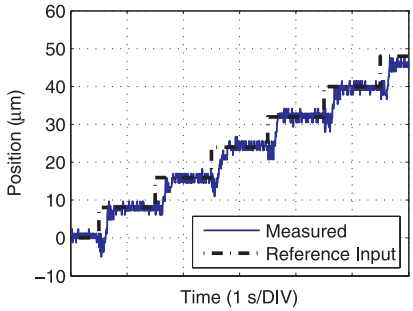
4. Measurement results

This measurement results are roughly divided in two parts. First, the performance of the position actuator will be analyzed. Then some characteristics of the haptic device, such as mechanical stiffness, performance in virtual reality example, and non-contact assistance, will be described.

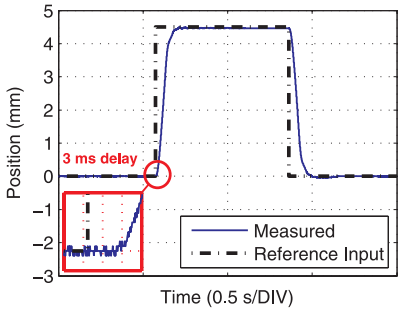
4.1. Position actuator performance

The performance of the position actuator is evaluated on four points: accuracy; response delay; repeatability, and how well the position output follows the reference input signal (servo behavior). For this purpose, the real displacement of the actuator measured by an external laser sensor (Keyence LC-2440).

The accuracy of the position actuator is measured by a step response of which the step height equal is to the position resolution (8 μm). The result of such an incremental step response is shown in Fig. 7(a), where the position actuator follows the reference input (dashed line) accurately. A larger step response is shown in Fig. 7(b) and it shows more clearly the limited maximum velocity of the actuator. The subplot indicates a time delay of 3 ms between the reference input and the real motion. The repeatability of the actuator is evaluated by



(a) Incremental step of 8 μm



(b) Step showing time delay and speed limitation

Fig. 7 Step response of stepper motor position actuator

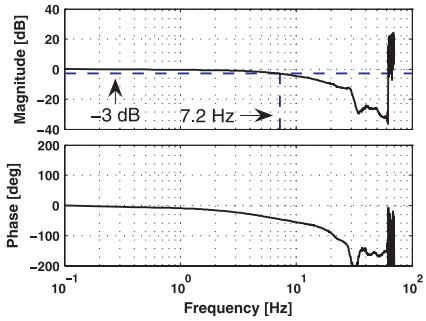


Fig. 8 Bode plot of position actuator

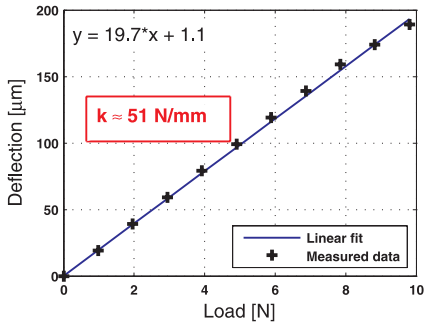


Fig. 9 Mechanical stiffness of SCARA structure

comparing the position value before and after the two step commands of Fig. 7(b). This error (not shown in the graph) is 5 μm and thus smaller than the step resolution.

The performance on servo behavior is analyzed by a multi-purpose FFT analyzer (Ono Sokki CF-5220), where the frequency range was set at 0.1-100 Hz. As an input signal, a 2 mm peak to peak sinusoidal reference signal was sent to the position actuator. The resultant Bode diagram is shown in Fig. 8. The bandwidth, here defined as the -3 dB crossing, is indicated at 7.2 Hz, which is sufficient to cover most of the human hand motion frequency range.

4.2. Mechanical stiffness

As the vertical stiffness is an important performance criterion of the haptic device, the performance in terms of stiffness is measured. The device itself has mechanical stiffness, which is a result of the structure of the kinematic chain, while there is also a virtual stiffness that can be set in the virtual model. The mechanical stiffness varies depending on the posture of the two links, but the lowest stiffness value can be expected when the two links are aligned and fully extended (Same posture as in Fig. 5). To measure the mechanical stiffness for this case, a load is applied to the end-effector using weights, while the deflection is measured by a laser displacement sensor. The result is shown in Fig. 9 and from the slope of the measurement, a mechanical stiffness of 51 N/mm is derived. This stiffness is sufficient as it satisfies the required 10^4 N/m order which is need for the application of non-contact handling using electrostatic levitation.

4.3. Virtual stiffness and viscosity

To demonstrate the performance of the haptic device in a virtual reality application, a simple virtual environment has been constructed in ControlDesk that will show the behavior of a point mass with a force applied to it (coming from the force sensor) and interacting with 3 different conditions, namely free air, a viscous environment, and a wall (stiff one-directional spring). This environment thus completely exists inside the virtual model and the conditions

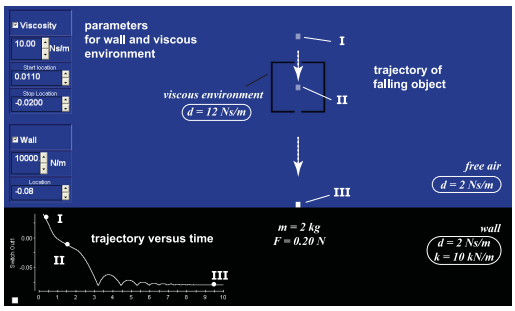


Fig. 10 Virtual 1DOF environment

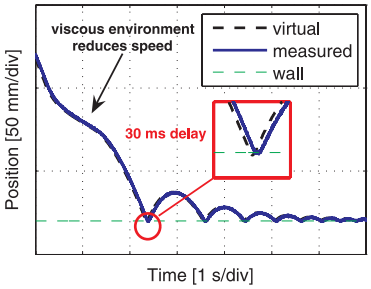


Fig. 11 Details of bouncing

are chosen such that the performance of the haptic device is shown. The situation that can be imagined is that an object, attracted by gravity, falls towards a surface. Before hitting this surface, the object is subjected to a viscous field, which damps the falling speed when the object is in this viscous environment. When the object finally hits the surface, a springlike interaction will bounce the object back from the surface repeatedly until it finally rests on this surface. This behavior is shown real-time on a computer screen and a final screenshot of it is shown in Fig. 10. Note that by photo editing software, remarks and annotations have been added. The initial position of the object is indicated by (I). The environment around this position has only damping 2 Ns/m and because of a constant input force to the force sensor, the object will accelerate down like a falling object. When the object is inside the viscous environment (II), indicated by the black brackets, the damping is much higher (12 Ns/m) and thus the speed of the falling object will reduce. After the viscous environment the object will bounce on the surface. This surface is indicated by the black color and basically it represents a very stiff one-directional spring, which in this case has a stiffness of 10 N/mm. Due to the damping in the free air environment and wall, the bouncing of the point mass on the wall reduces until it remains motionless on the wall (III). A plot of the virtual trajectory of the point mass versus time is real time displayed on the bottom left side where the three time instants I,II, and III are indicated. The location of the object at time instants I and II were added to the screenshot afterwards to increase comprehension of figure.

All parameters of this virtual environment, such as mass, viscosity, wall stiffness, location, etc. can be set directly in the application and they are also noted in the figure. The load force however is externally applied to the force sensor by attaching a small weight (mass 20 g) to the force sensor. Details of the point mass trajectory versus time are also measured by an external laser displacement sensor (NAiS LM10-ANR1215) and the results are given in Fig. 11, showing clearly the influence from the viscous environment and the bouncing behavior. It also shows a time delay of 30 ms between real output and virtual output, which is higher then the time delays found when only the position actuator was evaluated. This difference comes from the type of input signal that is sent to the position actuator. The time delay of 30 ms is a realistic value for the intended application of non-contact handling and does not pose a serious problem.

4.4. Non-contact handling of hard disk media

The application for which the haptic device is developed is to assist a human operator in handling sensitive objects such as silicon wafers without contact using electrostatic levitation. In a pilot experiment, successful handling (pick and place) has been realized, in which the haptic device performs as required and it will be reported in another publication. Instead of a silicon wafer however, an aluminum disk from a conventional 3.5” hard disk is used for the experiments as the cost is lower and it can easily be replaced if the experiment fails. As electrostatic levitation can levitate both conductors and semi-conductors, the same strategy is also valid for silicon wafers.

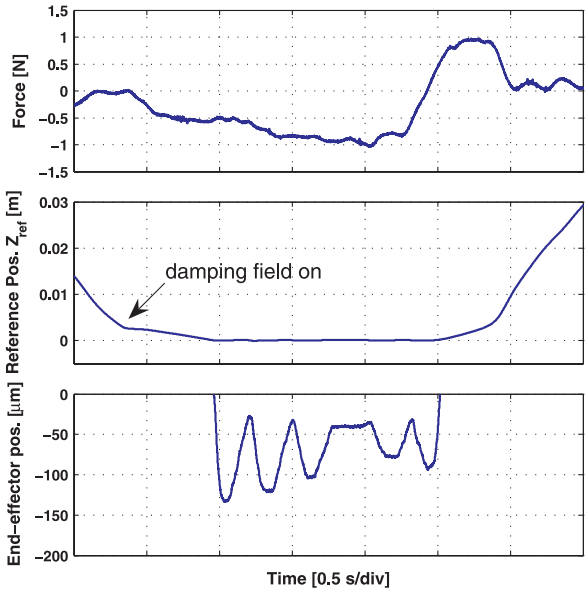


Fig. 12 Placing of object, end-effector does not exceed 150 μm

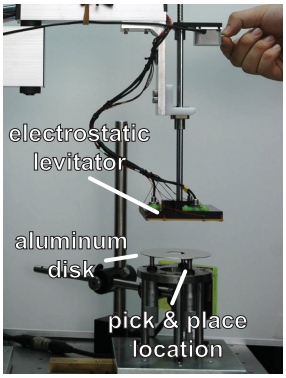


Fig. 13 Overview of human, haptic device, object (aluminum disk), and pick and place location

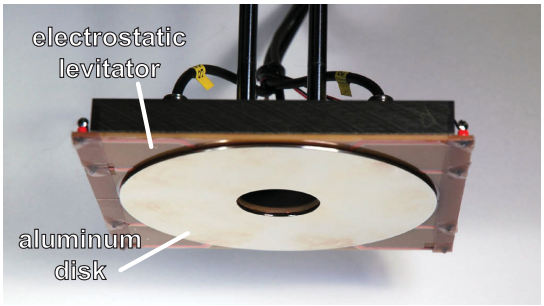


Fig. 14 Aluminium disk during stable levitation

In the experiment the human operator exerted a pick and place force in the order of 1 N (measured by force sensor of haptic device). During normal conditions, the air gap between object and levitator is about 350 μm as is also shown in Fig. 3(b). During the picking up and placing, this air gap is forced smaller. The stiffness from the haptic device however, prevented at all time that the air gap did not become smaller than 150 μm which means that stability was maintained. Data of a placing experiment showing force, reference position, and end-effector position at the critical moment are given in Fig. 12. The position is zero at the moment the object touches the desired location, so that the error can easily be read. A photograph of the setup and stable levitation is shown in Fig. 13 and Fig. 14. An additional proximity sensor (Keyence LC-2440) was used to trigger a high damping field as the levitator approaches the pick and place location in order to reduce the speed, which is also indicated in Fig. 12.

5. Conclusion

In this paper a new SCARA-type haptic device is presented that can be used in a collaborative system to improve the human performance in the non-contact handling of sensitive objects like silicon wafers. The admittance controlled haptic device has the general structure as the SCARA-type robot, of which only the vertical motion is actively controlled. The me-

chanical stiffness of the device for the vertical direction at its weakest configuration (the two links fully extended and aligned) is 51 N/mm and this satisfies the minimum requirement of 10^4 N/m order.

The position actuator that is used for creating the vertical motion is a direct ball screw stepper motor combination that has in controlled conditions a step resolution of 8 μm and a maximum speed of 80 mm/s. The bandwidth of the position actuator is 7.2 Hz, which is sufficient to perform in the haptic device for the non-contact object handling task.

The haptic device can accurately interact with a virtual environment, which has been demonstrated by displaying a falling object in different conditions, such as a viscous environment and hitting a virtual wall. The measured time delay between input to the position actuator and real output is 30 ms, which is larger than the time delay measured for a step response (3 ms), but still acceptable for the intended application. A pilot experiment showed that the performance of the device for non-contact handling, such as pick up and place is also sufficient.

Acknowledgements

This work was partly supported by a Grant-in-Aid for Scientific Research, No. 18360117, from MEXT in Japan.

References

(1) B. Hannaford, "A design framework for teleoperators with kinesthetic feedback," *IEEE Transactions on Robotics and Automation*, vol. 5, no. 4, pp. 426 – 34, Aug. 1989.

(2) T. H. Massie and J. Salisbury, "The phantom haptic interface: A device for probing virtual objects," in *Proc. of ASME Winter Annual Meeting, Symposium on Haptic Interfaces for Virtual Environment and Teleoperator Systems*, pp. 295–301, Nov. 1994.

(3) H. Kazerooni, "Human power amplifier technology at the university of california, berkeley," *Rob. Autom. Syst.*, vol. 19, no. 2, pp. 179 – 187, Dec. 1996.

(4) T. Nojima, D. Sekiguchi, M. Inami, and S.Tachi "The SmartTool: A system for augmented reality of haptics," in *Proc. Virtual Reality Annual International Symposium*, pp. 67–72, Mar. 2002.

(5) R. Taylor, P. Jensen, L. Whitcomb, A. Barnes, R. Kumar, D. Stoianovici, P. Gupta, Z. Wang, E. deJuan, and L. Kavoussi, "A steady-hand robotic system for microsurgical augmentation," *International Journal of Robotics Research*, vol. 18, no. 12, pp. 1201 – 1210, Dec. 1999.

(6) E. van West, A. Yamamoto, and T. Higuchi, "The concept of "haptic tweezer", a non-contact object handling system using levitation techniques and haptics," *Mechatronics*, vol. 17, no. 7, pp. 345 – 356, 2007.

(7) J. Jin, T. Higuchi, and M. Kanemoto, "Electrostatic levitator for hard disk media," *IEEE Transactions on Industrial Electronics*, vol. 42, no. 5, pp. 467 – 73, Oct. 1995.

(8) J. Jin, T. Higuchi, and M. Kanemoto, "Electrostatic silicon wafer suspension," in *Fourth International Symposium on Magnetic Bearings*, pp. 343 – 348, ETH Zurich, 1994.

(9) J. U. Jeon and T. Higuchi, "Electrostatic suspension of dielectrics," *IEEE Transactions on Industrial Electronics*, vol. 45, no. 6, pp. 938 – 46, Dec. 1998.

(10) S. Padhy, "On the dynamics of SCARA robot," *Robotics and Autonomous Systems*, vol. 10, no. 1, pp. 71 – 8, 1992.

(11) C. Clover, G. Luecke, J. Troy, and W. McNeely, "Dynamic simulation of virtual mechanisms with haptic feedback using industrial robotics equipment," in *Proceedings. 1997 IEEE International Conference on Robotics and Automation*, pp. 724 – 30, USA, 1997.

(12) R. van der Linde and P. Lammertse, "Hapticmaster - a generic force controlled robot for human interaction," *Industrial Robot*, vol. 30, no. 6, pp. 515–24, 2003.